Paper No.
2015-6396

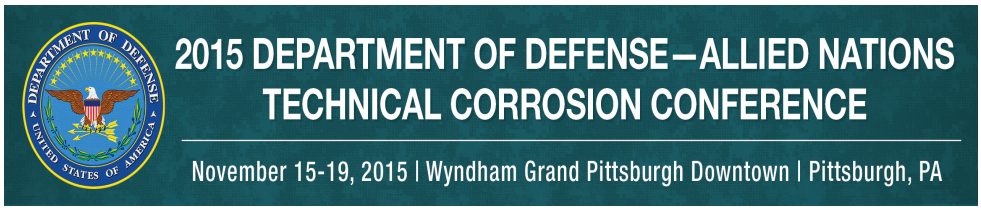

Study of Corrosion Pit to Fatigue Crack Transition in AA7075-T651 Aluminum Alloy

Justin W. Rausch, Scott A. Fawaz
SAFE Inc.
3290 Hamal Circle
Monument, CO 80132
United States of America

ABSTRACT

A test procedure is currently under development to investigate the effect of environment on the initiation and propagation of fatigue cracks. The goal is to create a test procedure that any reasonably equipped test lab could execute by following the sated procedures. Additionally the test protocol should create test data that can be directly compared from one test site to another. A common test procedure could lead to a greater sharing of data among research centers and aid in our collective understanding of the how nucleation of fatigue cracks from pits can be slowed or stopped. Major components of the test procedure include, methods to create lab generated corrosion pits that replicate observed damage, mechanical testing guidance for fatigue testing in both lab air and under various environments, and data collection, analysis, and interpretation of the results. The ultimate goal of this test methodology would be widespread acceptance as a standardized method for testing how various environmental factors influence crack nucleation and growth. The test procedures currently have proven to be capable of creating lab generated pits of tailored sizes, being able to consistently match fatigue crack growth rates in lab air, and capture the reduction of life and influence of environment on test specimens.

Key words: Fatigue, Pitting Corrosion, Mechanical Testing, Direct Current Potential Difference, Environmental Testing

INTRODUCTION

Pits in aircraft structure have long been known for their role in crack nucleation.[1] The two primary methods for maintaining the structural integrity of aircraft currently in use today, damage tolerance and safe life, treat these small cracks from pits differently. For a given crack that nucleates from a corrosion pit, the majority of its life is spent nucleating and growing in the short crack range.[2] These small cracks from pits pose little effect on the maintainers using damage tolerant design because the small crack growth mostly occurs in the time to reach the 0.05 in (0.1.27 mm) rogue flaw already assumed to be present in the material.[3] However, from a safe life perspective, knowing how fast cracks nucleate and propagate can factor significantly into how much useful life a component may have. Furthermore any change in coating or environment that may be more aggressive or beneficial may not be accounted for in the component life. To be conservative safe life uses the harsher environment to allow a crack to

grow to 0.25 mm.[4] Some chromate coatings have been shown to provide a reduction in crack growth rate over this range of crack growth. Conversely, some of the non-chromate primers and corrosion protection compounds have been shown to have a slightly higher crack growth rate in the same small crack growth regions.[5] The push for less toxic materials is changing the chemistry of some primers and the full consequences of the changes should be understood. This test protocol is designed to give researchers who test for these small changes in crack growth, testing and specimen preparation techniques to allow research and development to occur on a common platform.

EXPERIMENTAL PROCEDURE

There are three scenarios often encountered when evaluating corroded structures in aircraft. These three scenarios involve corrosion that starts from an open hole (for cases of lightning holes, drain holes, etc.), a filled hole (typically when fasteners are installed in components), or a surface flaw (normally found on the part surface away from any other geometry). Typically these areas account for the majority of corrosion damage found on modern aircraft. The proposed test protocol uses two specimen geometries designed to provide the researcher platforms to replicate damage found in service. In the following sections there will be further discussion about the development of each specimen and its impact on the total test package.

Test Specimen Development

Since the goal of the test program is to capture the effect environment has on the small crack behavior between samples in air and in varying environments, it was required to have a characterized material to reduce a potential source of variability. A previous test program provided sample material that was previously characterized by experimental test methods.[6] This SIPS (Structural Integrity Prognosis System) material and test data for 7075-T651 aluminum plate was subsequently used for all test samples due to its known mechanical properties and published crack growth data. The SIPS aluminum plate chemical composition is shown in Table 1.

Table 1
Composition of SIPS 7075-T651 aluminum plate

Element	Al	Zn	Mg	Cu	Fe	Cr	Si	Mn	Ti
Weight Percent (%)	89.55	5.70	2.53	1.66	0.26	0.19	0.06	0.03	0.02

Other relevant mechanical properties for the SIPS include tensile yield strength of 508 MPa (73.6 ksi), and plain strain fracture toughness (K_{IC}) 33 MPa$\sqrt{m}$ (30.03 ksi$\sqrt{in}$). Additionally crack growth rates are also known for varying thicknesses through the plate. All specimens used in this test program were fabricated from the material referenced above and taken from a thickness of T/6 from the plate. The first specimen designed was the open hole test specimen. This specimen was designed to replicate damage initiating from a corrosion pit that had been generated at the corner of the hole bore and free surface. Open holes are not normally found on aircraft for fatigue reasons, but the open hole provides a convenient and basic geometry that affords corrosive environment a direct influence on the pit. This intrusion from the environment into the pit is primary effect observed when a change in crack growth is measured. Mechanically speaking a well-designed specimen needed to be easy to manufacture, resistant to out of plane loads, and easy to model in the virtual space. A diagram of the open hole specimen is shown in Figure 1.

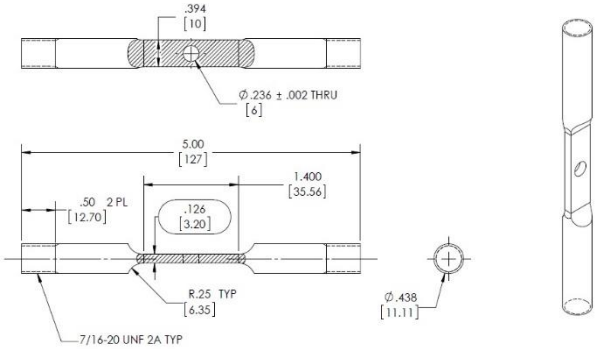

Figure 1: Schematic of the open hole specimen

The open hole design will also double for a filled hole or occluded test specimen in further test development. By simply installing a fastener inside the hole, the tester can tailor the experiment to add additional similitude to a representative structure. This includes designing specific environmental ingress for specific cell design, simulating changes in fastener fit, wet installed fasteners, or other experimental parameters. The second specimen was designed to mimic a crack that nucleates form a pit in the open surface of a part. This pitting scenario is commonly found in many types of structure such as thin skin, thick skin, secondary and primary structure. Any part that can corrode can be replicated by this design. The difficult part of flat surface pit specimen design is to protect against crack nucleation away from the pit. At small pit sizes, about 50µm in the "c" direction, the stress concentration due to the pit is approaching the stress concentrations of other small machining or handling defects. The small stress concentration puts added emphasis on the surface finish. Additionally part thickness, radius size, and test section shape are critical to drive the crack nucleation and initiation to the corrosion pit. Figure 2 shows a drawing of the flat surface specimen.

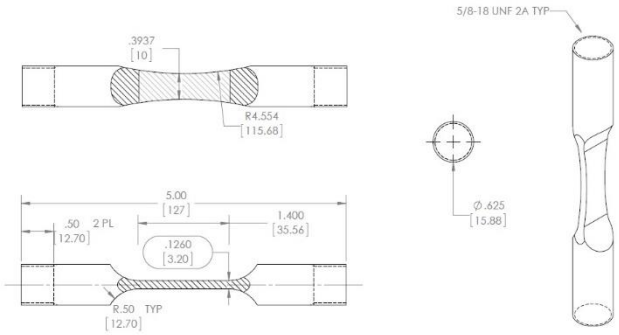

Figure 2: Flat surface specimen schematic

Pitting Procedure

Much of the pitting procedure was developed by Martra.[7] The quality of the lab generated pits was tested and compared to naturally occurring pits. The end result found that the lab generated pitting procedure successfully created pits of similar morphology when compared to naturally occurring pits observed on in-service components. To validate the lab generated pits, the surface morphology was compared to naturally occurring pits using Hirox stereo microscopy, SEM (Scanning Electron Microscope) microscopy, and confocal microscopy. All three methods confirmed that the lab produced pits had similar surface morphology when compared to the naturally occurring pits and judged the lab generated pits as a suitable replacement for naturally occurring pitting. The complete pitting procedure used to create pits is found in the reference list at the end of the paper, however a summary of the procedure steps are as follows:

1) Clean the area around where the pit will be placed.
2) Make a hole the same size as the desired pit in a piece of tape.
3) Adhere the tape with the hole centered on the desired pit location.
4) Mask off all areas of bare metal aside from the hole in the tape and an area for the constant current lead to be attached.
5) Submerge the specimen in the pitting solution
6) Turn on the current source
7) Allow electrochemical reaction to take place for the desired amount of time to produce desired pit size (A table relating current and desired size is shown in the full procedure)
8) Remove sample from solution and rise with water.

As the pitting process was refined the desired pit size became smaller in attempts to expand the pit size variable space. When attempting to make smaller sized pits, on the order of 150µm diameter or less, it was difficult to start the pitting process. The electro chemical circuit would appear to be open, resulting in no current flow through the exposed metal. It was theorized that the surface tension of the pitting solution was sufficiently high enough to prevent the wetting of the exposed metal underneath the hole in the tape. This would cause the exposed metal to be electrically insulated causing the open circuit. To reduce the surface tension of the solution, heating the pitting solution to approximately 60 degrees Celsius helped with the ease of creating the smaller diameter pits. Heating the solution allowed the formation of 50 µm diameter holes to be created with the standard pitting procedure. Surfactants were also considered, but were ruled out as to not influence the electro chemistry. Once pitted the specimens would be examined under the microscope to measure both the ‘a’ and ‘c’ dimensions of the pit. During pit measurement the ‘a’ and ‘c’ dimensions of the specimen are kept as close to perpendicular to the microscope as possible while still observing the pit. This allows the most accurate measurement, but will have some error associated with it. These measurements will be double checked, and corrected if needed, during post-test SEM fracture surface analysis. The pit measurements are recoded and used during testing as inputs in to the FTA (Fracture Technology Associates) crack growth software.

Spot-Welding Procedure

Platinum lead wires were used for the DCPD (Direct Current Potential Difference) sensing probes. Platinum wires provided a better corrosion resistance to the copper lead wires when immersed in solution. Like the pitting procedure, the entire spot welding protocol is published in reference eight.[8] An overview of the process is outlined below:

1) Affix specimen into the specimen holder under the microscope.
2) Clean the surface of the specimen and the leads of the platinum wire with alcohol or other degreaser to prepare the surface for welding.
3) Tape down the leads of the specimen near the pit.
4) Position platinum DCPD leads as near to the pit as possible without damaging the specimen surface near the pit.
5) Lower the spot weld probe into contact with the platinum wire
6) Fire the electric pulse.

The spot-welding process outlined above has additional settings for the spot-weld energy levels associated with each particular welder. The energy level setting outlined in the protocol may only work for the specified spot-welder. Placement of the DCPD leads is also critical. It has been shown that the most sensitive measurements require the probes to as close to the site of interest as possible with equally spaced leads.[9] The feasible spacing for the two specimen geometries were approximately 400-600 µm from the specimen centerline.

Test Procedure

Once the specimens have been pitted and the DCPD leads spot-welded, they are ready for mechanical testing. Specimens are threaded into two grips, with these grips then pinned to the clevises that attach to the load cell and ram of a servohydraulic test frame. The DCPD current leads are attached directly to the top and bottom grip. Figure 3 shows the typical test setup for both a lab air specimen and a specimen with the environmental chamber fitted.

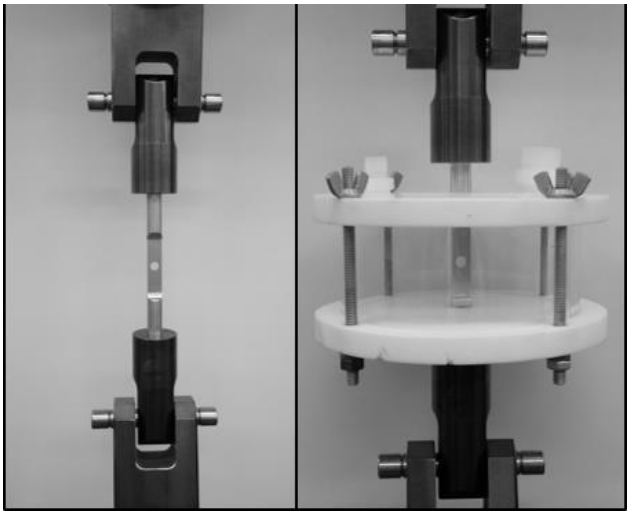

Figure 3: Open hole specimen test setup (Left) and open hole specimen in environment (Right)

Multiple stress levels were tested in lab air to determine an appropriate balance between initiation time and test length. Since the goal is to test the effect of environment on the crack growth and initiation from the pit, it is not efficient to run at very high stress levels as high stress levels will dramatically shorten the nucleation time and thusly the potential environmental impact. Previous testing experimented with 70 MPa (10.1 ksi), 125 MPa (18.1 ksi), and 180 MPa (26.1 ksi) stress levels. Based on this previous testing it was decided to use the 125 MPa stress level for the initial testing as it best balanced time to nucleation and failure. Table 2 shows the relative comparison of cycles to nucleation, periphery crack formation, and total cycles between applied stress levels.

Table 2
Comparison of number of cycles to nucleation, periphery crack formation and total cycles between three stress levels of the open hole specimens.

Specimen ID	Cycles to Nucleation (Marker Band Measurements)	Cycles to Periphery Crack Formation	Total Cycles
S70-1	665060	782480	906080
S70-2	765205	810072	930582
S70-3	1881617	1943417	2097917
125-1	10279	31709	60399
125-2	7073	25413	50523
125-3	11521	27539	48348
S180-1	< 250	7725	13101
S180-2	< 250	7210	16012
S180-3	< 250	10815	18216

Use of marker spectrum

A variable amplitude load spectrum was used during testing to create markers on the fracture surface of each specimen. After the fatigue test had completed each lab air specimen fracture surface was cleaned and sectioned in preparation for SEM measurements. Each specimen fracture surface was then analyzed under high and low magnification to count each of the markers back to initiation. Counting the number of markers observed back to the pit would provide the number of cycles from initiation to the end of the fatigue test. The shape of the crack was also tracked during the fracture surface analysis. The size of the crack was recorded when the crack becomes one complete front from the 'a' side to the 'c' side. This periphery crack gives additional insight into the crack growth. Prior to the periphery crack formation it is hard to make crack predictions as multiple small cracks are interfering with each other. This makes the prediction difficult. After the periphery crack formation prediction becomes much easier and accurate. The marker bands were used during all testing to provide positive identification of how the crack front was changing from initiation through periphery crack formation and through failure or test stoppage. To keep the load spectra consistent between tests the marker spectrum was also used for the full immersion tests as well as the lab air specimens. Post-test fracture analysis of the immersion samples found that the corrosive environment made marker band measurement difficult, with very few marker bands visible on the fracture surface. DCPD voltage will be used to acquire crack data for all immersion tests. One pass of the marker spectrum is comprised of 8170 cycles. The 8170 cycles was further broken down with three markers consisting of ten bands, four bands, and six bands. Figure 4 shows and example of one of the sets of marker bands. In this example there are six bands seen in the middle of the image bounded by the dotted lines.

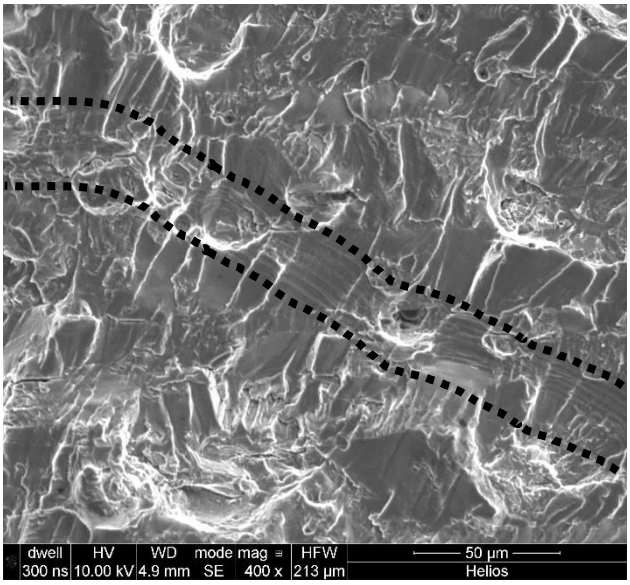

Figure 4: Example marker band (6)

RESULTS

Open hole lab air data

The first step in test methodology validation was the production of repeatable results from a known environment. Lab air was chosen as the simplest environment for the initial tests. The open hole samples were tested with the variable amplitude marker spectrum with a peak load of 4 kN (899 lbs.). The applied load resulted in a 125 MPa (18.1 ksi) peak remote stress level at the peak applied load.

Table 3 shows a comparison of crack data collected by DCPD and crack data collected by post-test marker measurements. The source of each measurement is given in parentheses in each column of data. For example, the fourth column is a list of the number of cycles to nucleation based on marker band measurements, where the fifth column is a list of the number of cycles to nucleation based on the DCPD voltage data.

Table 3
Comparison of open hole DCPD and marker band measurement results

Specimen ID	Normalized DCPD value at nucleation (DCPD data)	Normalized DCPD value at nucleation (Marker Band Measurements)	Cycles to Nucleation (Marker Band Measurements)	Cycles to Nucleation (DCPD Data)	Periphery Crack Dimension, a	Periphery Crack Dimension, c	Normalized DCPD Value at Periphery Crack (Marker Band Measurements)	Cycles to Periphery Crack Formation	Total Cycles
Open Hole Lab Air Specimens									
125-1	1.00004	1.00068	10279	9406	0.259	0.213	1.01832	31709	60399
125-2	1.00002	1.00146	7073	8608	0.249	0.119	1.00190	25413	50523
125-3	1.00023	1.00672	11521	14521	0.445	0.276	1.01850	27539	48348

At the 125 Mpa stress level the three specimens had a similar number of cycles to nucleation and total number of cycles until failure. Of note is how close the number of cycles to nucleation is between the two methods (DCPD data vs. Marker data). The close agreement between the two methods becomes important when the open hole specimen is tested in a corrosive environment. When testing in environment the corrosion attack can remove the markers forcing the test to rely solely on the DCPD voltage. The agreement between the number of cycles to nucleation based on the DCPD voltage and the number of cycles until nucleation based on the markers suggests that DCPD voltage trends allow for the identification of nucleation based on the DCPD data. Additional validation can be performed by a comparison of the crack growth rates obtained from the open hole test specimens against the crack growth rates published in the SIPS test program. Crack growth rate comparisons between open hole specimens 2 and 3 (da/dn vs. delta K was not calculated for the first sample) and published crack growth rate data from the SIPS program are shown in Figure 5.
.

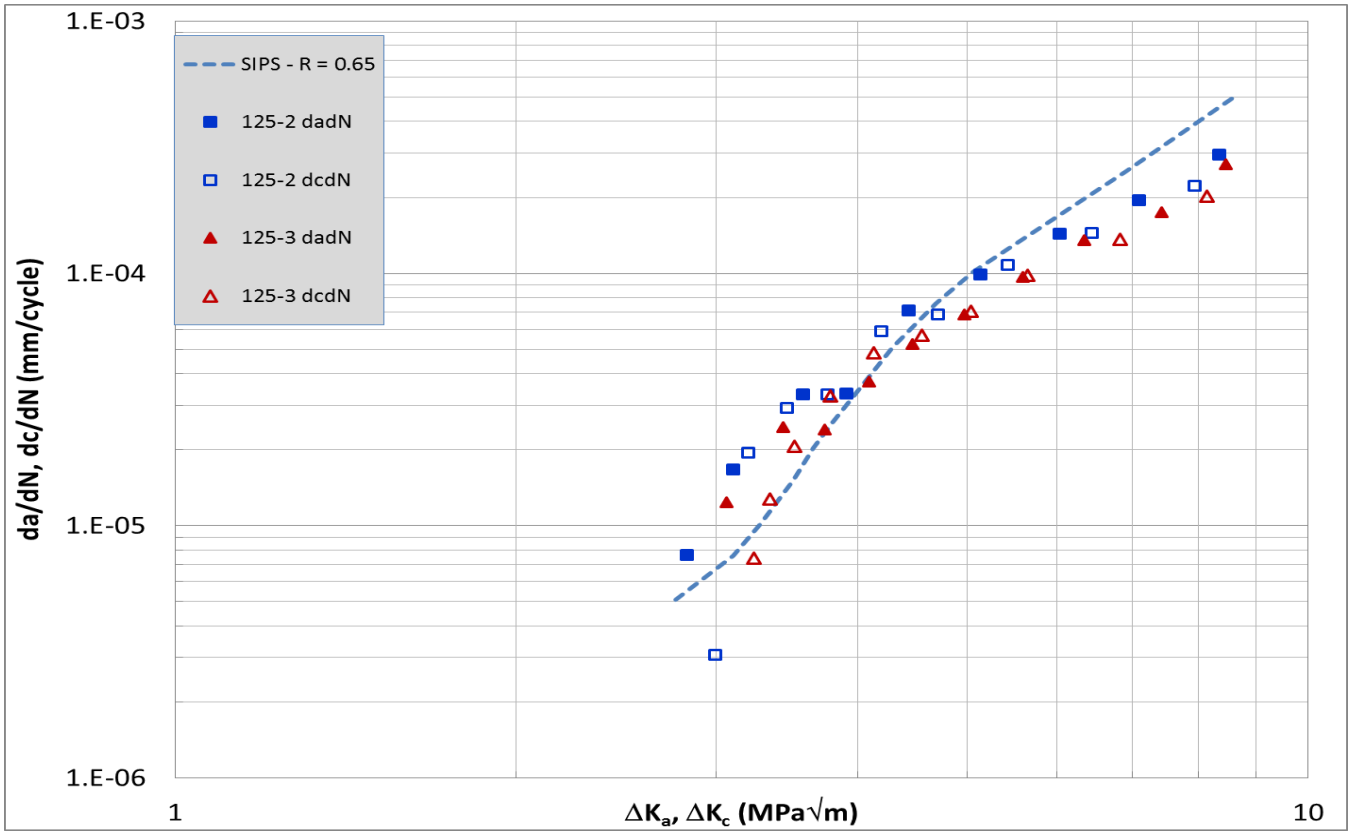

Figure 5: Crack growth rate comparison between lab air samples and published SIPS data

Crack growth rates from 125-2 and 125-3 closely match the published SIPS data. The open hole specimens have slightly higher crack growth rates below ΔK of approximately 4 MPa√m and crack growth rate slightly lower above 4 MPa√m. Some amount of scatter can begin to be seen as ΔK goes below 4 MPa√m toward threshold, however the two specimens behave very similar as expected when testing in low humidity lab air.

Flat surface pit lab air data

Validation of the flat surface pit specimen data followed the same steps as the open hole specimens. The first step in validation of the flat surface pit specimens was to produce repeatable results in lab air. The flat surface pit tests were performed in lab air just like the open hole specimens. Flat surface pit specimens were tested with the same variable amplitude marker spectrum except that the peak load was increased to 13.1 kN (2945 lbs). The applied load resulted in a 410 MPa (59.5 ksi) peak remote stress level at the peak applied load. The higher applied load was required as there was no additional geometry contributing to the stress intensity factor like the hole in the open hole specimens. Table 4 shows a comparison of data collected by DCPD and data collected by marker measurements.

Table 4
Flat surface pit lab air data

Specimen ID	Cycles to Nucleation, indicated by DCPD Data	Total Cycles
410-1	5500	58285
410-2	85000	139375
410-3	1740	246504

At the 410 MPa stress level the three specimens had varying number of total cycles and cycles to nucleation among the three test specimens. The variability in the data can be traced back to the corrosion pit size. The pit size is formed as a function of current and time, and with the current held constant during the pitting process the only variable changing is time. The current pitting process uses a stopwatch to measure the amount of time that has passed when creating the pit. The problem becomes apparent when small amounts of hydrogen gas build up and insulate the pit stopping the pitting process. Accounting for the stopped pitting time is difficult as the visual cue is fast fluctuating source voltage while the electrochemical cell is open. While the cell is open no pitting is taking place, requiring judgment to be used to decide how much time has passed while the circuit was open. A future enhancement is to build a more robust method to accurately time the amount of time the circuit is closed and generating a pit. To measure the effect of the pit size variability AFGROW (Air Force Growth) was used to predict the change in cycles to failure based on the pit size.[10] A simple model was created that replicated a pit in the cross-section of flat surface pit specimen. The pit size was varied to model each of the three specimens, and a constant amplitude stress of 410 MPa was applied. Table 5 shows the measured pit size for each of the 410 MPa specimens along with the cycles to failure and AFGROW predicted cycles to failure.

Table 5
Comparison of pit size actual and predicted cycles to failure

Specimen ID	Pit Size, a (µm)	Pit Size, c (µm)	Cycles to Failure (Actual)	Cycles to Failure (Predicted)
410-1	70.8	82.9	58285	113200
410-2	52.6	88.4	139375	123900
410-3	32.3	53.6	246504	211200

From Table 5 the increase in life with decrease in pit size is evident. As the pit size became smaller between specimen 1 and 3 the specimen life went up accordingly. AFGROW does not predict nucleation time, and as such under predicts the life. At the high stress levels required to nucleate from the small pit tiny changes in geometry can have large effects on the remaining life. In future work tighter control of the pit size will be required. Just like the open hole specimens corrosion can remove the markers forcing the test to rely solely on the DCPD voltage. The agreement between the number of cycles to nucleation based on the DCPD voltage and the number of cycles until nucleation based on the markers suggests is currently being evaluated. Similar to the open hole specimens the crack growth rate data generated from the flat surface specimens will be validated against the published SIPS crack growth rates.

CONCLUSIONS

Open hole lab air samples created and tested with the protocols have shown good agreement with previously published results. The crack growth rates between published SIPS data and the open hole specimens show good correlation. Additionally the open hole lab air specimens were shown to be repeatable. A combination of high required stress and variation in pit size were shown to be cause of significant fluctuation in the nucleation and total cycle counts on the flat surface specimens. Tightening of control processes during pitting resulted in more consistent results.

Future Work

The present work comprised of two geometries tested in lab air conditions. Test results in lab air are driven by the material with very little effect from the environment. Future work will focus on testing the

precision and results of the test procedures in other environments. Full immersion testing in a corrosive environment (0.06M NaCl solution) of both sample geometries is currently in work. Initial results are showing the expected decrease in specimen life but data quality is suffering because the spot-welded leads are also exposed to the environment. This work will also be augmented by an occluded specimen geometry. Further work will add inhibitors into solution to add additional test criteria to the results.

ACKNOWLEDGEMENTS

The author would like to thank the Office of Naval Research, for their continued funding and support. Thanks are also due to the Center for Aircraft Structural Life Extension at the United States Air Force Academy for use of the lab facilities.

REFERENCES

1. Wei, R.P., et al. (1997), “CORROSION AND CORROSION FATIGUE OF ALUMINUM ALLOYS: CHEMISTRY, MICROMECHANICS AND RELIABILITY”, AFSOR Grant No. F49620-93-1-0426, LEHIGH UNIVERSITY,Bethlehem, PA

2. J. Schijve, Fatigue of Structures and Materials, 2nd ed. (Springer Science+Business Media, B.V. 2009), p. 22.

3. Joint Service Specification Guide, Aircraft Structures, JSSG-2006, United States Department of Defense, 30 October 1998.

4. Fixed Wing Aircraft Structural Life Limits, Instruction 13120.1. (1997) Naval Air Systems Command.

5. Gasem, Z and R.P. Gangloff, “Rate Limiting Proceses in Environmental Fatigue Crack Propagation in 7000-series Aluminum Alloys”, Chemistry and Electrochemistry of Corrosion and Stress Corrosion Cracking (2001); p. 501-521.

6. Papazian, J., Anagnostou, E. L., Christ, R. J., et al. (2009), “DARPA/NCG Structural Integrity Prognosis System”, HR0011-04-C-0003. DARPA, Arlington, VA.

7. Mantha, D. USAFA-TR-2013-04, Pitting Protocol, Center for Aircraft Structural Life Extension (CAStLE), USAF Academy, CO 80840, (2013).

8. Mantha, D. USAFA-TR-2013-05, Spot Welding Protocol, Center for Aircraft Structural Life Extension (CAStLE), USAF Academy, CO 80840, (2013).

9. R.P. Gangloff, “Electrical Potential Monitoring of Crack Formation and Subcritical Growth from Small Defects”, Fatigue of Engineering Materials and Structures (1981); p. 15–33.

10. Harter J.A., AFGROW Users Guide and Technical Manual Version 5.02.01.18, LexTech Inc, Centerville, OH